On the phase transition in N-isopropylcarbazole

R. Nowak and E. R. Bernstein

On the phase transition in *N*-isopropylcarbazole

R. Nowak[a] and E. R. Bernstein

Department of Chemistry, Condensed Matter Sciences Laboratory, Colorado State University, Fort Collins, Colorado 80523

The elastic properties of *N*-isopropylcarbazole (NIPC), a pyroelectric molecular crystal, are investigated by Brillouin scattering. The full elastic constant tensor is determined at 295 K and the temperature dependences of the elastic constants are given. The major experimental finding reported is the anomaly of the LA *a*-axis mode governed by the c_{11} elastic constant. This mode exhibits a pronounced downward bending on both sides of the nonferroic, first order phase transition at ~ 137 K. Symmetry allowed linear-quadratic and biquadratic couplings between the Brillouin zone boundary one-dimensional order parameter and the zone center strain introduced into the Landau free energy do not account for the observed anomaly. The transition is characterized in terms of a strong dispersion of the c_{11} elastic constant and a large dynamical critical behavior. By combining the c_{11} elastic constant data and the Brillouin scattering LA *a*-axis mode half-width data through a Landau–Khalatnikov process, one can extract a relaxation time satisfying a mean-field dependence characteristic of critical slowing down of the order parameter.

I. INTRODUCTION

N-isopropylcarbazole (NIPC) is a pyroelectric molecular crystal exhibiting strong tribo-[1] and pyroluminescent[2,3] properties associated with the polar structure of the crystal. A structural phase transition in NIPC at ~ 137 K, taking place between the C_{2v}^{21} (*Iba*2) high temperature structure and the C_{2v}^5 (*Pbc*2$_1$) low temperature structure, has been reported in the literature.[4,5] Dilatometric,[4] pyroelectric,[2,4] and specific heat[6] measurements reveal the first order character of this transition. The enthalpy of the transition is found to be $\Delta H^T = 125$ cal mol^{-1}, a value higher than most displacive[7] or even order–disorder[8] phase transitions in molecular crystals. Calorimetric measurements[6] reveal an additional anomaly of the specific heat around 185 K, indicating the possible existence of another (non-first-order) phase transition.

Very little is known about the mechanism of the NIPC phase transition at 137 K. From the symmetry point of view, NIPC is a rare example of a molecular crystal exhibiting a phase transition without any point symmetry breaking; only the translational symmetry changes at the transition (the volume of the primitive unit cell doubles in the low temperature phase). Chloranil[9,10] is another well known example of such a nonferroic[11] phase transition among organic solids.

A group theoretical analysis of the transition in NIPC suggests that the transition takes place at the Brillouin zone boundary[5] and that the order parameter transforms according to a one-dimensional representation of the group of the wave vector (only one vector of the star of the wave vector is involved in the transition). Bilinear coupling of the order parameter to macroscopic quantities at the zone center (e.g., strains) is thus forbidden by symmetry. The lowest order coupling permitted by symmetry is then a third order non-

linear interaction. Although this kind of transition does not involve new macroscopic tensor components below the phase transition, anomalies of the elastic constants may arise due to the higher order couplings, as is the case for chloranil.[10]

The molecular mechanism of the phase transition in NIPC is not completely clear. Recent crystallographic data[5] have shown large librational motion of the NIPC molecules at room temperature. In particular, libration around the molecular axis of largest moment of inertia exhibits surprisingly large amplitude (7.1°), at least twice the amplitude of the two other principal axis librations. The amplitudes of the librations become almost equal and significantly smaller in the low temperature phase and only small rotation–translation shifts of the molecules occur at the transition. The carbazol group of the molecule itself is planar in both phases. The only significant change in molecular geometry at the phase transition is a rotation of the isopropyl group around the C–N bond by an angle of 14° and 10° for layers I and II, respectively.[5] These results show that the phase transition in NIPC does not affect the molecular conformation in an essential way: the phase transition may be considered as an order–disorder or rotation–translation coupling type transition. Rotation–translation coupling, as well as "freezing" of the orientational motion of molecules in the low temperature phase, has been previously reported to characterize phase transitions in such molecular crystals as *s*-triazine,[12] benzil,[13] and chloranil.[10]

As was already mentioned, the NIPC crystal is pyroelectric, and thus also piezoelectric, in both phases. The molecular dipole moments are directed along the C–N bonds of the molecules which are oriented about the direction of the twofold *c* axis; the spontaneous polarization of the crystal is, therefore, parallel to this axis. Due to the piezoelectric coupling, dielectric and elastic anomalies cannot be separated, in general. Therefore, some of the observed elastic constants must be corrected by[14]

---

[a] On leave from the Institute of Organic and Physical Chemistry, Technical University of Wrocław, 50-370 Wrocław, Poland.

$$\bar{c}_{\alpha\beta} = c_{\alpha\beta} - e^2_{k\alpha\beta}/\epsilon_k$$

in which $c_{\alpha\beta}$ is a bare elastic constant, $e_{k\alpha\beta}$ is a piezoelectric constant, and ϵ_k is a bare dielectric constant. Since the anomalous part of the dielectric constant of NIPC is much smaller than its normal part,[4] the main effect of the piezoelectric coupling is to shift the absolute values of the elastic constants. If this coupling is ignored, one can separate interactions between the order parameter and strains from interactions between the order parameter and polarizations.

In this report we present a complete study of Brillouin scattering in NIPC at 1 atm pressure between 295 and $\sim$100 K. The elastic constant tensor is determined and the temperature dependences of the elastic constants are given. The observed anomaly of the a-axis longitudinal acoustic phonon associated with the e_1 strain is discussed on the basis of Landau mean-field theory and interpreted in terms of a Debye relaxation–dispersion of the elastic constant.

II. EXPERIMENTAL PROCEDURES

Single, transparent crystal boules of NIPC ($\sim$5 cm^3 in volume), exhibiting a [100] perfect cleavage plane and [010] nonperfect one, are grown from the melt using a Bridgman technique.[15] Oriented crystals are cleaved with a razor blade and/or cut with a wire saw into parallelepiped shaped samples $\sim$4$\times$4$\times$3 mm. The saw-cut faces are polished on a tissue soaked with ethyl acetate. In order to reduce surface scattering and prevent sample sublimation during experiments, crystal faces are coated with a thin layer of silicon oil prior to the experiment.

Right angle scattering experiments are performed using three different kinds of samples characterized by different orientations: (1) faces perpendicular to the three crystallographic axis—this orientation allows for measurements of phonons in the directions [110], [101], and [011]; (2) faces oriented 45° with respect to the crystallographic axes in the ab plane—phonons in the directions [100] and [010] can be measured in this orientation; and (3) faces oriented 45° with respect to the crystallographic axes in the ac plane—either [100] or [001] phonons can be obtained.

The Brillouin scattering apparatus, including measuring techniques and temperature control, used in these experiments has been described previously.[12,13] A Spectra Physics model 165 argon ion laser, operating at 5145 Å (200 mW) in a single cavity mode is used for the scattering source. Spectra are obtained with a Burleigh Fabry–Perot interferometer system in triple-pass operation with a standard finesse of 45 to 50. To analyze the spectra and to record the temperature dependences of the acoustic phonons, free spectral ranges between 15 to 30 GHz are chosen. Typically, 50 or 100 accumulations of a 1 s duration scan are stored and averaged in a multichannel analyzer and computer.

III. RESULTS

The velocity of sound v in an optically anisotropic crystal can be calculated by[16]

$$\omega_B = \frac{2\pi v}{\lambda_0}(n_i^2 + n_s^2 - 2n_i n_s \cos\theta_s)^{1/2} \tag{1}$$

in which n_i, n_s are the refractive indices for incident and scattered light, respectively, λ_0 is the incident light wavelength in vacuum, and θ_s is the scattering angle (90° for right angle scattering). Thus, knowing the frequency shift (ω_B) and the polarizations of the incident and scattered light from the experiment, one can easily calculate the sound velocity, providing refractive indices of the crystal are known.

The refractive indices of NIPC are measured at 5145 Å by a prism minimum deviation method. The accuracy of this method in our case is only slightly better than 5%; the error is mostly due to the poorly determined geometry of the prisms and the quality of their surfaces. The values of the refractive indices are subsequently verified and adjusted by comparing their ratios to the ratios of the Brillouin shifts measured along the principal axes in backscattering geometry for different polarizations. Refractive indices obtained in this way and used for calculations of sound velocities are $n_a = 1.846$, $n_b = 1.648$, $n_c = 1.664$. Elastic constants of NIPC are calculated using the density $\rho = 1.15\times10^3$ kg^{-3} taken from x-ray data.[5]

A. Determination of the elastic constants at room temperature

Elastic constant tensor and piezoelectric constant tensor for both orthorhombic phases of NIPC are given by

$$\begin{bmatrix} c_{11} & c_{12} & c_{13} & 0 & 0 & 0 \\ c_{12} & c_{22} & c_{23} & 0 & 0 & 0 \\ c_{13} & c_{23} & c_{33} & 0 & 0 & 0 \\ 0 & 0 & 0 & c_{44} & 0 & 0 \\ 0 & 0 & 0 & 0 & c_{55} & 0 \\ 0 & 0 & 0 & 0 & 0 & c_{66} \end{bmatrix}$$

and

$$\begin{bmatrix} 0 & 0 & 0 & 0 & e_{15} & 0 \\ 0 & 0 & 0 & e_{24} & 0 & 0 \\ e_{31} & e_{32} & e_{33} & 0 & 0 & 0 \end{bmatrix},$$

respectively. The equation of motion for the piezoelectric crystal is of the form

$$(\bar{c}_{ijkl} - \rho v^2 \delta_{ik})u_k^0 = 0 \tag{2}$$

in which

$$\bar{c}_{ijkl} = c^E_{ijkl} + \frac{(e_{pij}m_p)(e_{qkl}m_q)}{\epsilon^s_{jk}m_j m_k} \tag{3}$$

are the elastic constant coefficients modified by the piezoelectric coupling, and the m's are the direction cosines. The solutions of the equations of motion corresponding to the phonons observed in our experiments are shown in Table I. Additional terms of the form of Eq. (3) in the Table describe the change of the velocity of those phonons which couple to the electric field via piezoelectric coupling. As already mentioned in the Introduction, the dielectric properties of NIPC do not show a large anomaly at the phase transition.[4] As a result, interactions between the order parameter and strains can be, in principle, separated from interactions between the order parameter and polarizations. Thus, only the shifts of absolute values of the elastic constants will be considered in the determination of the elastic constant tensor and its tem-

TABLE I. Solutions of the equation of motion for NIPC. Only modes observed in the experiments are included in the table. [See Eqs. (2) and (3) in the text.]

Phonon direction	Polarization	$X_i = \rho v^2$
[100]	L [100]	$X_1 = C_{11}$
	T [010]	$X_2 = C_{66}$
	T [001]	$X_3 = C_{55} + e^2{}_{15}/\epsilon_{11}$
[010]	L [010]	$X_4 = C_{22}$
	T [100]	$X_5 = C_{66}$
[001]	L [001]	$X_6 = C_{33} + e^2{}_{33}/\epsilon_{33}$
	T [100]	$X_7 = C_{55}$
[110]	qL [110]	$X_8 = 1/4\{C_{11} + C_{22} + 2C_{66} + [(C_{11} - C_{22})^2 + 4(C_{12} + C_{66})^2]^{1/2}\}$
	qT [1$\bar{1}$0]	$X_9 = 1/4\{C_{11} + C_{22} + 2C_{66} - [(C_{11} - C_{22})^2 + 4(C_{12} + C_{66})^2]^{1/2}\}$
	T [001]	$X_{10} = 1/2[C_{44} + C_{55} + (e_{15} + e_{24})^2/(\epsilon_{11} + \epsilon_{22})]$
[101][a]	qL [101]	$X_{11} = 1/4\{C_{11} + C_{33} + 2C_{55} + [(C_{11} - C_{33})^2 + 4(C_{13} + C_{55})^2]^{1/2}\}$
	qT [10$\bar{1}$]	$X_{12} = 1/4\{C_{11} + C_{33} + 2C_{55} - [(C_{11} - C_{33})^2 + 4(C_{13} + C_{55})^2]^{1/2}\}$
[011][a]	qL [011]	$X_{13} = 1/4\{C_{22} + C_{33} + 2C_{44} + [(C_{22} - C_{33})^2 + 4(C_{23} + C_{44})^2]^{1/2}\}$
	qT [01$\bar{1}$]	$X_{14} = 1/4\{C_{22} + C_{33} + 2C_{44} - [(C_{22} - C_{33})^2 + 4(C_{23} + C_{44})^2]^{1/2}\}$

[a] Piezoelectric coefficients are omitted in these two instances because they complicate the expressions considerably and do not significantly alter the form of the expression as given.

perature dependence. Values of these shifts cannot, however, be calculated from Eq. (3) due to lack of experimental data.

On the other hand, the change of the acoustic mode velocity due to the piezoelectric coupling can be estimated[17] from the electromechanical coupling coefficients k_{ij}: specifically, $c^{eff} = c/(1 - k^2)$. Preliminary measurements[15] have shown that $k_{31} = 0.15$, $k_{32} = 0.18$, $k_{24} = 0.11$: k_{33} and k_{15} could not be measured due to weak piezoelectric signals. Employing these values of the electromechanical coupling coefficients, the largest change in the sound velocity caused by piezoelectric coupling is estimated to be 1.6%. Thus, the experimentally observed elastic constants c differ from bare elastic constants by less than $\sim 3\%$. The piezoelectric coupling will not be included in the ensuing discussion, as it is of little importance to the elastic anomalies.

The values of the elastic constants of NIPC are calculated using the appropriate relations from Table I. c_{11}, c_{22}, c_{33}, c_{55}, and c_{66} are obtained directly from X_1, X_4, X_6, X_3 and X_7, X_2, and X_5, respectively, with an accuracy of $\sim 2\%$. As we are not able to detect the transverse mode governed by the c_{44} elastic constant directly, its value is determined from the velocity of the TA phonon propagating in the [110] direction using relation X_{10}. The off-diagonal elements of the elastic tensor c_{12}, c_{13}, and c_{23} are calculated from the relations $X_8 - X_9$, $X_{11} - X_{12}$, and $X_{13} - X_{14}$, respectively. Their values are determined with a relatively large error ($\sim 30\%$) due to the combination of the elastic constants in the em-

ployed equations, as well as to the relatively small values of the off-diagonal elements. The room temperature set of elastic constants found in the above manner is given in Table II.

Angular sound velocity diagrams can be calculated from the values of the elastic constants given in Table II. These diagrams, given in Fig. 1, reflect the anisotropic nature of the crystal structure. The c_{11} elastic constant which governs the velocity of the [100] LA phonon is relatively large, whereas the molecular interactions in this direction, which is perpendicular to the cleavage plane, are expected to be weak.

B. Temperature dependences of the elastic constants

The temperature dependences of the six diagonal elastic constants are shown in Figs. 2–4. The c_{22}, c_{44}, and c_{55} elastic constants exhibit the step-like changes expected for a first order phase transition. Only a small effect is seen for the temperature dependence of c_{33}. An interesting anomaly around the phase transition at 137 K is found for the c_{11} elastic constant, which involves the e_1 strain in the crystal and governs the propagation of the LA phonon in the [100] direction. Figure 5 shows the temperature development of the [100] LA-mode spectrum; the other mode seen in this figure is the [100] TA mode governed by the c_{55} elastic constant. The Brillouin peak corresponding to the [100] LA phonon in the spectrum exhibits considerable broadening at the phase transition. The latter phenomenon typically indicates a higher sound attenuation at the phase transition, possibly due to the critical fluctuations. The temperature dependences of the half-width of this Brillouin peak and its intensity are shown in Fig. 6.

The anomalous temperature dependence of the c_{11} elastic constant shown in Fig. 2 may be fit using a phenomenological power law equation of the form

TABLE II. Room-temperature elastic constants of NIPC determined using relations displayed in Table I. The units are 10^9 N m^{-2}.

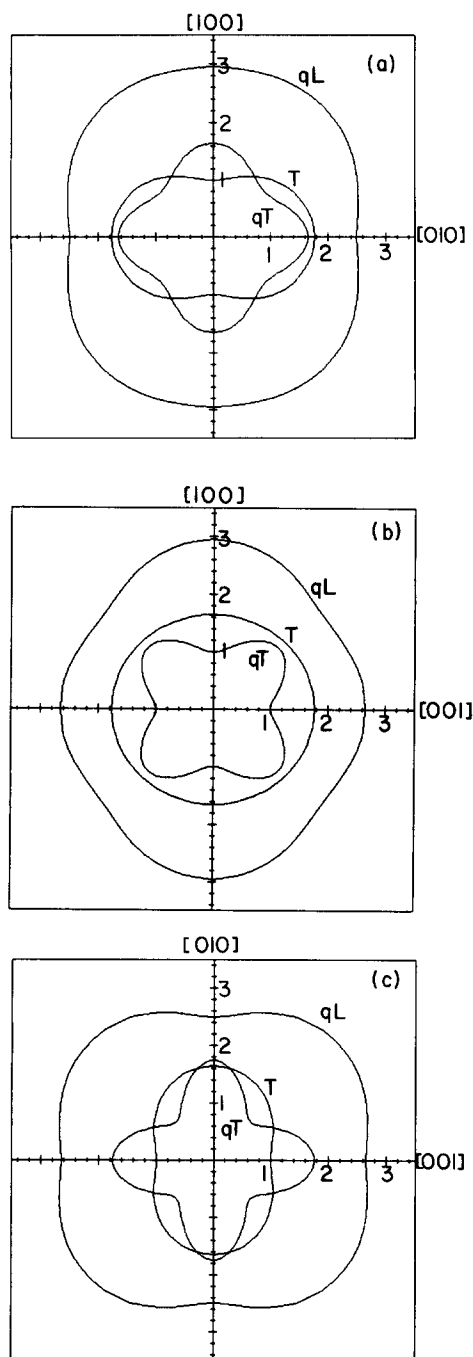| C_{11}	C_{22}	C_{33}	C_{44}	C_{55}	C_{66}	C_{12}	C_{13}	C_{23}
10.03	7.15	8.08	3.56	1.14	3.13	5.1	3.4	5.6

FIG. 1. Polar plots of the sound velocity of different acoustic modes in the ab (a), ac (b), and bc (c) planes of NIPC obtained using the nine independent elastic constants listed in Table II. The lines are calculated using the general solutions of the equation of motion, Eq. (2). Particular solutions in the directions of the crystallographic axes and diagonals are given by relations from Table I. The units are 10^3 m s^{-1}.

$$c_{11}(T) = c_{11}^0 - aT - be^{-\rho} \qquad (4)$$

in which the linear temperature term accounts for the behavior of the elastic constant in the absence of a phase transition and the last term represents the form of the critical anomaly. In Eq. (4) $\epsilon \equiv (T - T_0/T_0)$ or $\epsilon \equiv (T_0 - T/T_0)$ for the high and low temperature phases, respectively. The values of the parameters which give the solid lines in Fig. 2 are $c_{11}^0 = 15.11 \times 10^9$ N m^{-2}; $a = 1.5 \times 10^{-2}$ N m^{-2} K^{-1}, $b = 0.35 \times 10^9$ N m^{-2}, $T_0 = 135.5$ K, and $\rho = 0.67$ for the

high temperature phase, and $c_{11}^0 = 17.19 \times 10^9$ N m^{-2}, $a = 1.5 \times 10^{-2}$ N m^{-2} K^{-1}, $b = 2.05 \times 10^9$ N m^{-2}, $T_0 = 140.8$ K, and $\rho = 0.26$ for the low temperature phase.

Temperature dependences of the c_{12}, c_{13}, and c_{23} elastic constants cannot be obtained directly; however, they may be estimated from the temperature dependences of the modes propagating along the diagonal directions [110], [101], and [011] (see Table II). The temperature behavior of these modes is given in Fig. 7. Calculating the temperature dependences of c_{12}, c_{13}, and c_{23} according to the previously described procedure employed in the determination of their room temperature values, one finds that the off-diagonal elastic constants do not show any particular anomalous behavior at the phase transition. In other words, the temperature dependences of the diagonal elastic constants, c_{11} in particular, fully account for the anomalies shown in Fig. 7. The temperature dependences of the c_{66} and consequently c_{12} elastic constants cannot be determined in the low temperature phase due to cracking of the sample at the phase transition. In fact, several samples are used to obtain most of the temperature dependences shown in this paper.

Elastic constant anomalies which could confirm the existence of another phase transition at ~ 185 K, suggested on the basis of calorimetric measurements,[6] are not observed. Nonetheless, a change in slope of the temperature dependence of c_{11} is found near 185 K.

IV. DISCUSSION

The present Brillouin scattering study reveals the softening of the [100] LA mode governed by the c_{11} elastic constant, both above and below the phase transition at 137 K. Simultaneously a $\sim 200\%$ increase of the attenuation (halfwidth) of this phonon occurs at the transition. To explain these experimental findings, the Landau mean-field theory and dispersion–relaxation processes will be considered.

A. Landau free energy

Consider the group-theoretical analysis of the C_{2v}^{21} $\rightarrow C_{2v}^5$ phase transition in NIPC. In the Brillouin zone of the high temperature structure (Γ_0^v), five symmetry lines possess the C_{2v} point symmetry, appropriate to the considered transition;[18] however, only three points of this symmetry $k_\Sigma = (2\pi/a, 0.0)$, $k_\Delta = (0, 2\pi/b, 0)$, and $k_\Lambda = (0.0, 2\pi/c)$, all located at the Brillouin zone boundary, give doubling of the primitive unit cell volume at the transition. Thus, the transition takes place at the Brillouin zone boundary. As the star of the wave vector has only one arm and is nondegenerate, the order parameter (e.g., optical phonon) driving the transition belongs to a one-dimensional irreducible representation at the zone boundary.

Employing standard group theoretical methods,[19] the Landau free energy may be expressed in terms of the order parameter (η) as

$$G_\eta = (1/2)A(T)\eta^2 + (1/4)B\eta^4 + (1/6)D\eta^6 + \cdots \qquad (5)$$

in which $A(T) = a(T - T_0)$ stands for harmonic restoring forces of the optical mode. The elastic part of the energy is

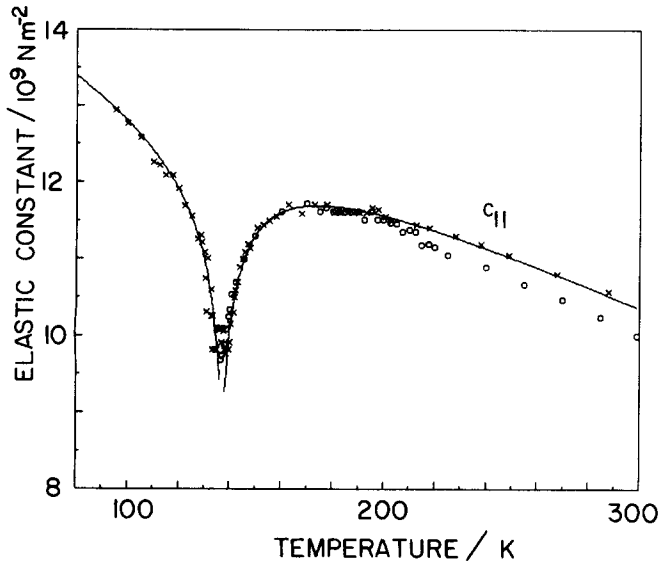$$G_{el} = (1/2)\Sigma_{\alpha\beta} c_{\alpha\beta} e_\alpha e_\beta \qquad (6)$$

FIG. 2. Temperature dependence of the c_{11} elastic constant. (O), (×) correspond to two different experimental runs performed using the samples of different orientations. The two runs are normalized at 190 K. The lines represent fits to the phenomenological Eq. (4), as well as to Eqs. (20) and (21), with the values of the parameters given in the text.

FIG. 4. Temperature dependences of the c_{44}, c_{55}, and c_{66} elastic constants: (O) and (×) correspond to two independent experimental runs.

The solution of the Hamiltonian including only the third order nonlinear coupling is already known in the literature for the phase transitions in terbium molybdate[20] and chloranil.[10] The theory predicts a continuous downward displacement of the elastic constant below the transition,

in which only the term $G_{el} = (1/2)c_{11}e_1^2$ will be considered because only the c_{11} elastic constant exhibits anomalous behavior in NIPC.

As the bilinear coupling between the zone boundary order parameter and the zone center strains is symmetry forbidden, the lowest order couplings which may be considered are a third order nonlinear interaction and a biquadratic coupling. Thus, the free energy interaction term is represented by

$$G_{e_1\eta} = -(1/2)(Ke_1\eta^2 + Le_1^2\eta^2).$$ (7)

The total Landau free energy is then of the form

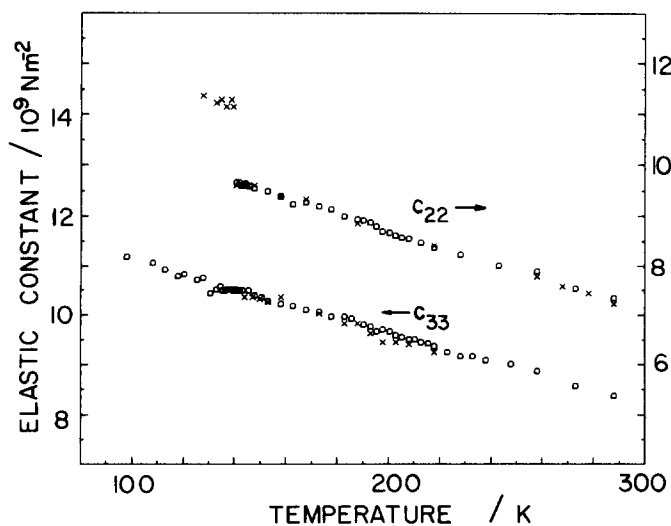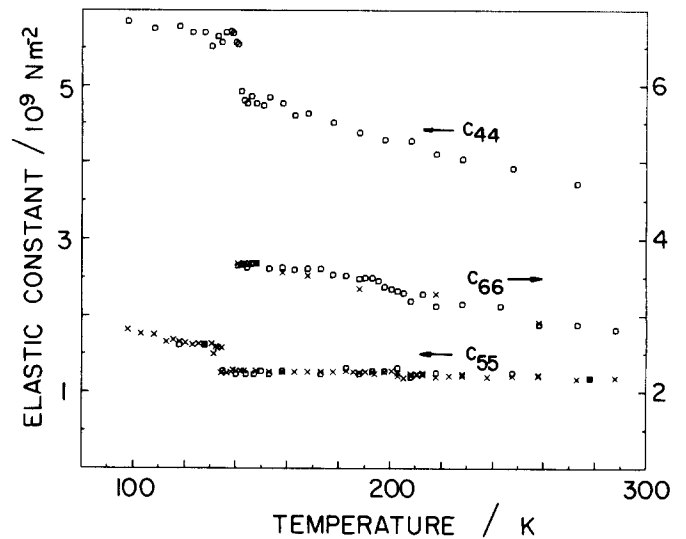$$G = (1/2)A(T)\eta^2 + (1/4)B\eta^4 + (1/6)D\eta^6 + (1/2)c_{11}e_1^2 - (1/2)Ke_1\eta^2 - (1/2)Le_1^2\eta^2.$$ (8)

FIG. 3. Temperature dependences of the c_{22} and c_{33} elastic constants: (O) and (×) represent different experimental runs.
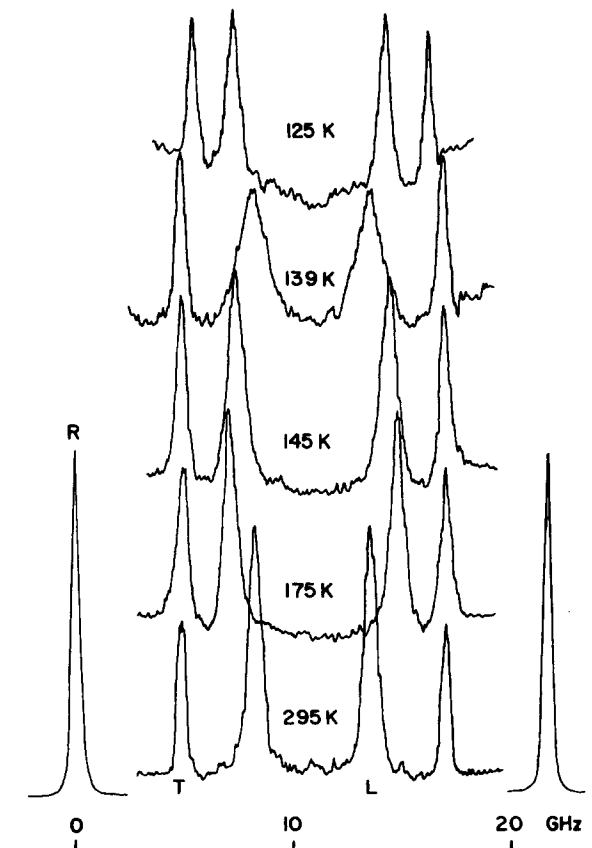

FIG. 5. The temperature development of the NIPC Brillouin spectrum due to [100] phonons. The free spectral range is 21.8 GHz. The longitudial and transverse modes, labeled L and T, respectively, correspond to the Rayleigh peak marked R. The spectra are taken in right angle scattering ($\theta = 90°$) in triple-pass.
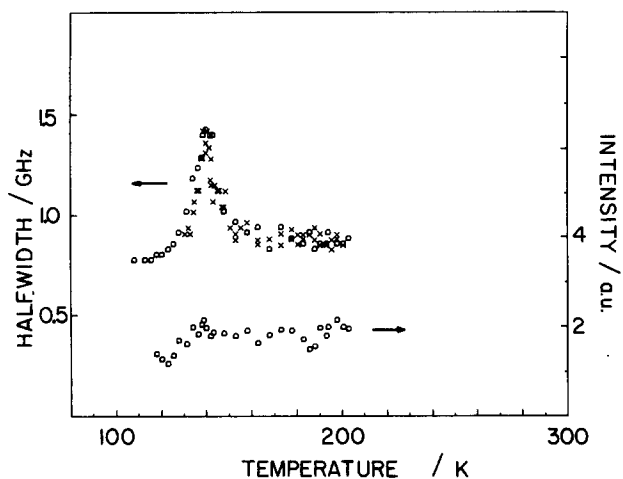
FIG. 6. Temperature dependence of the Brillouin half-width at half-maximum for the Brillouin feature corresponding to the [100] LA mode in Fig. 5. The half-width was not deconvoluted with respect to the width of the Rayleigh peak. (O) and (×) correspond to the two independent experimental runs. The lower points represent the temperature dependence of the Brillouin intensity of the same Brillouin feature taken as the area underneath the peak.

whereas above the transition the elastic constant is unaffected by the coupling.[20] In the case of NIPC the solution has the form

$$c_{11} = \begin{cases} c_{11}^0 & (T > T_0) \\ c_{11}^0 - \dfrac{K^2}{2B + 4D\tilde{\eta}^2} & (T < T_0) \end{cases} \qquad (9)$$

in which $\tilde{\eta}$ represents the equilibrium value of the order parameter in the low-temperature phase.

The equilibrium values of the order parameter $\tilde{\eta}$ and strain $\tilde{e}_1$, including both linear-quadratic and biquadratic interactions as in Eq. (7), are obtained by setting the generalized forces equal to zero

$$X_1 = \left(\frac{\partial G}{\partial e_1}\right)_\eta = 0, \quad \left(\frac{\partial G}{\partial \eta}\right)_{e_1} = 0, \qquad (10)$$

yielding

$$A(T) + \left(B - \frac{K^2}{c_{11}^0 - L\tilde{\eta}^2}\right)\eta^{-2}$$

$$+ \left(D - \frac{LK^2}{(c_{11}^0 - L\tilde{\eta}^2)^2}\right)\tilde{n}^4 = 0 \qquad (11)$$

and

$$(c_{11}^0 - L\tilde{\eta}^2)\tilde{e}_1 - (1/2)K\tilde{\eta}^2 = 0. \qquad (12)$$

Equation (12) has been used to eliminate e_1 from Eq. (11). In order to ensure that the transition is of the first order (which is appropriate for NIPC), $[B - K^2/(c_{11}^0 - L\tilde{\eta}^2)]$ must be negative.

B. The c_{11} elastic anomaly

Within the framework of the Landau theory, an effective elastic constant is calculated by a set of equations[21]

$$\frac{\partial G}{\partial \eta} = 0; \quad \frac{\partial G}{\partial e_1} = X_1 = c_{11}e_1. \qquad (13)$$

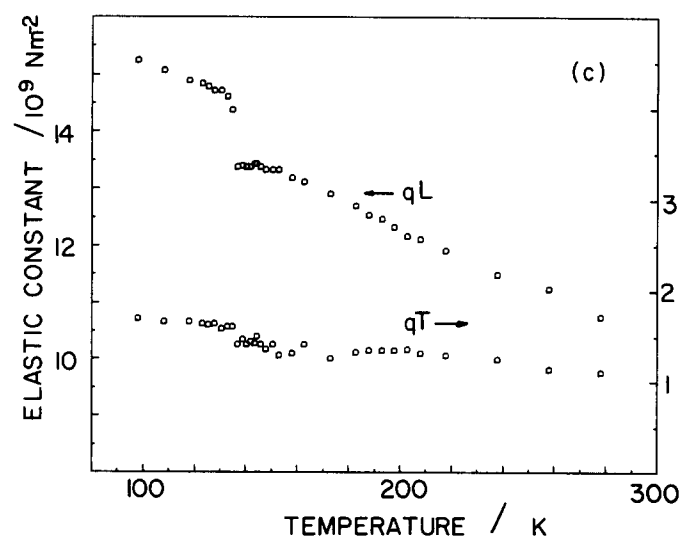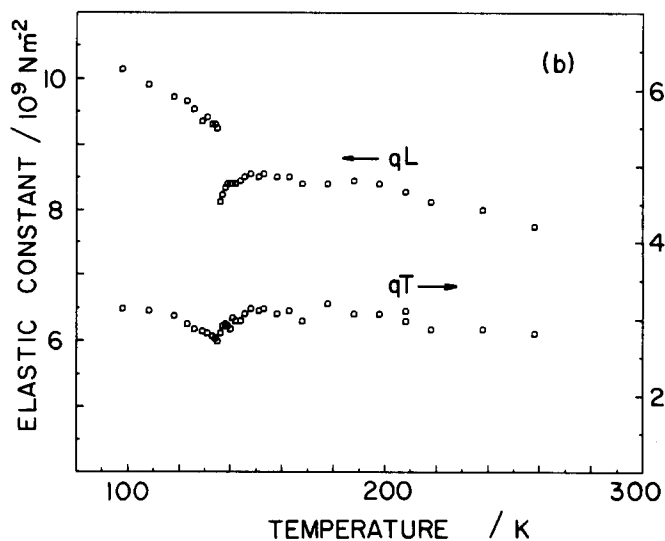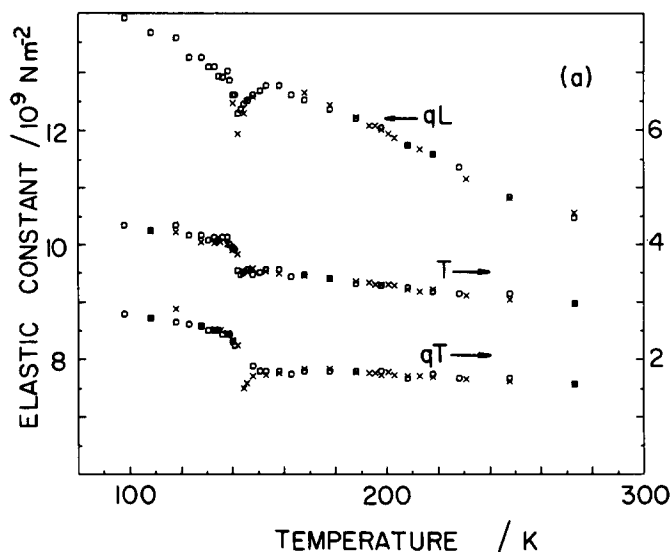Using the prescription of Eqs. (13) and (8) gives

FIG. 7. Temperature dependence of the effective elastic constants corresponding to [110] (a), [101] (b), and [011] (c) acoustic phonons specified in Table I. (O) and (×) correspond to different experimental runs.

$$\frac{\partial G}{\partial \eta} = [A(T) - Ke_1 - Le_1^2]\eta + B\eta^3 + D\eta^5 = 0 \qquad (14)$$

and

$$\frac{\partial G}{\partial e_1} = (c_{11} - L\eta^2)e_1 - (1/2)K\eta^2 = X_1 . \qquad (15)$$

In the high symmetry (high temperature) phase the strain and the order parameter possess only fluctuations, hence in Eqs. (14) and (15) $\eta = \delta\eta$ and $e_1 = \delta e_1$. Employing the standard procedure, the c_{11} elastic constant becomes

$$c_{11} = c_{11}^0 \quad \text{for } T > T_0$$

in which c_{11}^0 is the background elastic constant which linearly increases with decreasing temperature.

In the low symmetry (low temperature) phase η and e_1 possess spontaneous values $\tilde{\eta}$ and $\tilde{e}_1$ given by Eqs. (11) and (12). The order parameter and strain can then be described by small fluctuations $\delta\eta$ and δe_1 around the equilibrium values $\tilde{\eta}$ and $\tilde{e}_1$, and thus,

$$\eta = \tilde{\eta} + \delta\eta; \quad e_1 = \tilde{e}_1 + \delta e_1 .$$

Equations (14) and (15) can be written to linear order in fluctuations as

$$[A(T) + 3B\tilde{\eta}^2 + 5D\tilde{\eta}^4 - K\tilde{e}_1 - L\tilde{e}_1^2]\delta\eta$$
$$- (K\tilde{\eta} + 2L\tilde{e}_1\tilde{\eta})\delta e_1 = 0 , \qquad (16)$$

$$(c_{11}^0 - L\tilde{\eta}^2)\delta e_1 - (K\tilde{\eta} + 2L\tilde{e}_1\tilde{n})\delta\eta = X_1 . \qquad (17)$$

From this set of equations the elastic constant is found to be

$$c_{11} = c_{11}^0 - L\tilde{\eta}^2 - \frac{(K\tilde{\eta} + 2L\tilde{e}_1\tilde{\eta})^2}{A(T) + 3B\tilde{\eta}^2 + 5D\tilde{\eta}^4 - K\tilde{e}_1 - L\tilde{e}_1^2} . \qquad (18)$$

Using Eq. (14) in the above expression, one finds

$$c_{11} = c_{11}^0 - L\tilde{\eta}^2 - \frac{(K + 2L\tilde{e}_1)^2}{2B + 4D\tilde{\eta}^2} \qquad (19)$$

in which $\tilde{\eta}$ and $\tilde{e}_1$ are the equilibrium values given by Eqs. (11) and (12). The above thermodynamic treatment which includes linear-quadratic and biquadratic coupling terms in the free energy [Eq. (8)] gives only discontinuous downward displacement of the elastic constant below the transition. Thus, higher order interactions do not explain the experimentally observed "softening" of c_{11} shown in Fig. 2. These anharmonic terms further seem to be of little importance even close to the transition at which point critical fluctuations in η become large. These calculations indicate that the explanation of the critical behavior of the c_{11} elastic constant should be sought elsewhere; in particular, the dynamics of the system must be considered.

C. Other mechanisms

As mentioned above, the linear-quadratic and biquadratic couplings between the order parameter and the zone center elastic modes do not affect the elastic properties within the Landau theory in the high temperature phase. The situation in the crystal is more complicated for the case of NIPC and other mechanisms which can at least in part contribute to the observed anomaly of the [100] LA phonon should be mentioned. Among these are (1) anharmonic k-dependent

interactions between the [100] LA mode and fluctuations of the order parameter, (2) a soft zone center optical mode which couples to the acoustic mode, (3) a mean field Landau–Khalatnikov contribution, and (4) dispersion of the elastic constant.

Anharmonic coupling to critical fluctuations of the order parameter $\langle\eta^2\rangle$ may lead to a rounding of the discontinuity in c_{11} for $T > T_0$ and generate an additional contribution in the low temperature phase.[10,20] This mechanism accounts partially for the critical behavior in chloranil[10], terbium molybdate,[20] and ABO_3 perovskites.[22] The coupling of a soft optical mode at the Brillouin zone center to the mode causing the transition at the zone boundary is also a possibility. Coupling between strains and temperature dependent Raman-optical modes provides a satisfactory explanation for the elastic behavior in s-triazine[12] and the dependence of the qTA mode in chloranil.[10] A mean field Landau–Khalatnikov[23] contribution associated with the dispersion of the elastic constant can contribute to the elastic behavior in the low temperature phase as a rounding and restoring of the elastic constant. This mechanism is known to account partially for the behavior in layered perovskite compounds.[24]

Although the above mentioned mechanisms can all contribute to the anomaly of the c_{11} elastic constant, especially in the vicinity of the phase transition, they cannot entirely account for the observed behavior. Thus we find them possible but not likely. As will be argued in the next section, the most reasonable explanation of the behavior of the [100] LA phonon in NIPC is based on a dispersion–relaxation mechanism.

D. Dispersion of the elastic constant and dynamical mechanisms

One possible explanation of the critical behavior of c_{11} is that the elastic constant exhibits a frequency dependent relaxation which undergoes critical slowing down in the vicinity of the phase transition ($T = 137 \pm 40$ K). We propose a semiquantitative interpretation of the phase transition in NIPC based on this assumption. Since no ultrasonic or neutron scattering data are available for NIPC, the detailed mechanistic dynamics cannot be treated in much detail. Measurements of the [100] LA-mode velocity by a piezoelectric "resonance–antiresonance" method[6,15] give a value of 2150 m s^{-1} at room temperature. The velocity is almost 30% lower than the velocity obtained by Brillouin scattering (2953 m s^{-1}). In the former method the velocity is measured at the frequency of a standing acoustic wave ($\sim$90 kHz), whereas in Brillouin scattering the velocity is measured at a frequency of $\sim$12 GHz. The difference in the sound velocities measured by these methods is definitely outside the contribution from usual dispersion effects, typically less than 3%, and certainly much larger than the experimental errors. [A small difference (of the order of 1%) can be associated with these two experimental techniques due to the conditions of the experiment: adiabatic for Brillouin scattering and isothermal for the resonance–antiresonance method.] Moreover, the temperature dependence of the sound velocity obtained by both methods given in Fig. 8 shows a slight suppression of the critical behavior in Brillouin scat-
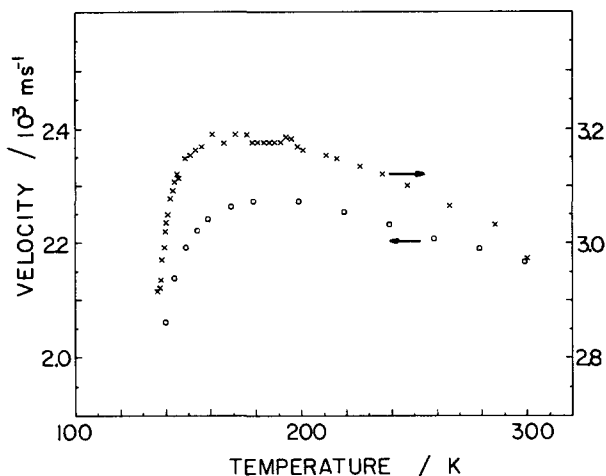
FIG. 8. Temperature dependences of the sound velocity of the [100] LA mode obtained by Brillouin scattering (crosses) at a frequency 12 GHz and resonance–antiresonance method (circles) at a frequency 90 kHz. The scales are slightly shifted with respect to one another for easy comparison.

tering. In order to confirm the difference in the sound velocities at room temperature, we have additionally performed ultrasonic pulse-echo experiments at a frequency of 10 MHz. The velocity of the [100] LA mode at 10 MHz is 2250 m s^{-1}.

The above experimental findings clearly suggest that dispersion/relaxation and its critical behavior at the phase transition are important for the elastic properties of NIPC. Moreover, the change of the attenuation at the transition indicates that some dynamical relaxation process is involved in this behavior. One possible mechanism for such a relaxation effect would be a dipolar orientational-relaxation process. From the standpoint of a "ferroelectric" phase transition, the anomaly in NIPC could be represented as an order–disorder transition of the permanent dipole moments of the individual molecules. This mechanism remains in agreement with the gradual freezing of the librational motions of molecules observed in the x-ray measurements[5] and with the temperature dependence of the spontaneous polarization.[4]

The most straightforward way to treat the frequency dependence in the high temperature phase is to assume a Debye relaxator form for the elastic constant:

$$c_{11}(\omega) = c_{11}(\infty) - \Delta c_{11}\left(\frac{T-T_0}{T_0}\right)^{-\rho} \Big/$$

$$[1 + (\omega\tau)^2] - aT, \qquad (20)$$

in which $\tau = \tau_0(T - T_0/T_0)^{-\nu}$. A good fit of the experimental results in Fig. 2 to this equation may be obtained with parameters: $c_{11}(\infty) = 15.11\times10^9$ N m^{-2}, $\Delta c_{11} = 0.61\times10^9$ N m^{-2}, $T_0 = 135.5$ K, $\rho = 1.01$, $\nu = 0.44$, $(\omega\tau_0)^2 = 1$, and $a = 1.5\times10^{-2}$ N m^{-2} K^{-1}.

In the low temperature phase a restoring of the c_{11} elastic constant is expected as temperature decreases from T_0. The increase in c_{11} can be expressed in a manner similar to the critical softening of Eq. (20),

$$c_{11}(\omega) = c'_{11}(\infty) - \Delta c'_{11}\left(\frac{T_0-T}{T_0}\right)^{-\rho'} \Big/$$

$$[1 + (\omega\tau')^2] - aT \qquad (21)$$

in which $\tau' = \tau'_0(T_0 - T/T_0)^\nu$. The parameters which give a good fit of Eq. (21) to the observed behavior in the low temperature phase are $c'_{11}(\infty) = 17.19\times10^9$ N m^{-2}, $\Delta c'_{11} = 3.96\times10^{-9}$ N m^{-2}, $T_0 = 140.8$ K, $\rho' = 0.43$, $(\omega\tau'_0)^2 = 1$, $\nu' = 0.27$ and $a = 1.5\times10^{-2}$ N m^{-2} K^{-1}. If one expands Eqs. (20) and (21) in a power series in $(T - T_0)/T_0$ and $(T_0 - T)/T_0$, respectively, Eq. (4), previously used for fitting the data, obtains. The fits of Eqs. (20) and (21) to the data are not completely unique because of the number of available parameters. Consequently, a, T_0, $c_{11}(\infty)$, and $c'_{11}(\infty)$ are chosen to correspond to the appropriate values obtained by fitting the phenomenological Eq. (4) to the data. Moreover, since for Brillouin scattering typically $\tau_0\omega \sim 1$ near the transition, $\tau_0\omega \equiv 1$ in the above procedure. Nonetheless, the values of $\Delta c_{11}, \rho$, and ν are not completely determined and similar quality fits can be obtained for small ($\pm 20\%$) variations of all three parameter values.

As shown in the case of barium sodium niobate,[25,26] the relaxation time may be obtained by combining the temperature dependence of c_{11} (Fig. 2) and the increase of the mode attenuation (displayed in Fig. 6) with a Debye form for the dispersion. Employing the theory of a complex elasticity with a single relaxation time,[13] one may write the elastic constant as

$$c_{11}(\omega) = c_{11}(\infty) - \frac{\Delta c_{11}}{1-\omega\tau(T)}. \qquad (22)$$

Separating Eq. (22) into real and imaginary parts yields

$$\rho v_{[100]}^2 = \text{Re } c_{11} = c_{11}(\infty) - \frac{\Delta c_{11}}{1 + [\omega\tau(T)]^2} \qquad (23)$$

and

$$\Gamma_{11}(T) = \Gamma_\infty + \frac{\Delta c_{11}\tau(T)}{1 + [\omega\tau(T)]^2}\frac{q^2}{2\pi\rho}. \qquad (24)$$

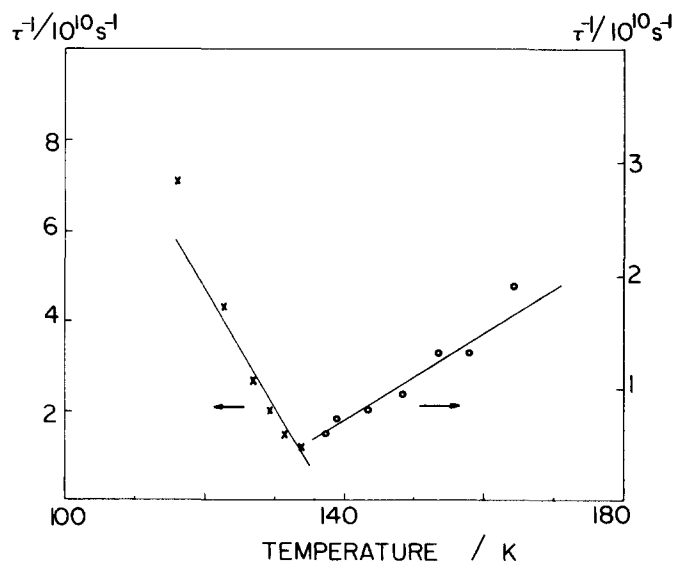By combining these two equations one obtains a very simple expression for the relaxation time

FIG. 9. Temperature dependence of the inverse relaxation time associated with the c_{11} elastic constant. Solid lines are the least squares fits to Eqs. (24) and (26) in the high and low temperature phase, respectively.

$$\tau(T) = \frac{\Gamma_{11}(T) - \Gamma_{\infty}}{c_{11}(\infty) - c_{11}(T)} \frac{2\pi\rho}{q^2}. \qquad (25)$$

Equation (25) is valid even if the relaxation time and coupling are wave vector dependent, since it involves data from a single frequency ω and wave vector q. Figure 9 shows the inverse of the relaxation time as a function of temperature. The line in the high temperature phase is of the form

$$\tau^{-1}(T,q) = \left|\frac{T - T_0}{T_0}\right| \tau_1^{-1} + \tau_2^{-1}(q). \qquad (26)$$

The fit to this equation gives $\tau_1 = 1.16 \times 10^{-12}$ s and $\tau_2 = 1.08 \times 10^{-10}$ s. In the low temperature phase

$$\tau'^{-1}(T,q) = \left|\frac{T_0 - T}{T}\right| \tau_1'^{-1} + \tau_2'^{-1}(q) \qquad (27)$$

with values of the coefficients $\tau_1' = 2.4 \times 10^{-12}$ s and $\tau_2' = 1.07 \times 10^{-10}$ s. The above temperature dependences of the relaxation times satisfy the prediction of a mean field critical slowing of the order parameter fluctuations in the vacinity of T_0.

V. CONCLUSIONS

The elastic properties of NIPC in the temperature range 90–295 K have been investigated by Brillouin scattering. In particular, the nonferroic, first order phase transition at ~ 137 K has been examined. Our findings can be summarized as follows:

(1) The c_{11} elastic constant associated with the [100] LA phonon exhibits an anomaly extending ~ 40 K above and below the phase transition at 137 K. The anomaly has the form of a softening of the c_{11} elastic constant; c_{11} falls to a minimum value in the transition region. The half-width at half-maximum of the [100] LA phonon also possesses anomalous broadening around the transition temperature.

(2) The c_{22}, c_{44}, c_{55}, and most likely also c_{66} elastic constants exhibit a step-like anomaly at ~ 137 K characteristic of a first order transition. Practically no anomalous behavior is observed for the c_{33} elastic constant. Only weak anomalies for the c_{12}, c_{13}, and c_{23} elastic constants are found.

(3) Sound velocity diagrams in the three crystallographic planes are calculated at room temperature using the values of the elastic constants determined in our experiments.

In order to explain the anomalous behavior of the c_{11} elastic constant two possibilities are considered: (1) an elaboration of the Landau theory with the inclusion of the linear-quadratic and biquadratic couplings between the zone boundary order parameter and zone center elastic strain; and (2) dispersion of the elastic constant combined with a temperature dependent relaxation process.

The c_{11} anomaly cannot be understood within the framework of the Landau theory which can only account for the downward discontinuous change of c_{11} at the transition. The anomaly can be understood by assuming dispersion of the elastic constant, possibly due to some relaxation process. This dynamical approach is justified by experimental find-

ings: a large difference in the velocity of the [100] LA phonon measured by experimental techniques employing different frequency domains; and suppression of the critical behavior at high frequencies (~ 12 GHz). In the framework of this latter approach the experimental data are reproduced using a power law equation including a term due to the assumed Debye relaxation behavior. The temperature dependence of the relaxation time is calculated by combining the temperature dependences of the elastic constant and attenuation. This behavior is found to satisfy the mean field dependence characteristic of critical slowing down.

[1] R. Nowak, A. Krajewska, and M. Samoć, Chem. Phys. Lett. **94**, 270 (1983).

[2] R. Nowak and R. Poprawski, Ferroelectrics Lett. **1**, 175 (1984).

[3] Z. Dreger, J. Kalinowski, R. Nowak, and J. Sworakowski, Chem. Phys. Lett. **116**, 192 (1985).

[4] R. Nowak, J. Sworakowski, R. Kowal, J. Dziedzic, and R. Poprawski, Ferroelectrics **65**, 79 (1985).

[5] F. Baert, A. Mierzejewski, B. Kuchta, and R. Nowak, Acta Crystallogr. Sect. B **42**, 187 (1986); the room temperature structure has been also reported by O. Saravari, Acta Crystallogr Sect. C **40**, 1617 (1984).

[6] M. Bertault, A. Collet, and R. Nowak, Solid State Commun. **58**, 613 (1986).

[7] H. Chihara and K. Masukane, J. Chem. Phys. **59**, 5397 (1973); I. Atake and H. Chihara, Solid State Commun. **35**, 131 (1980).

[8] J. L. Baudour, H. Cailleau, and W. B. Yelon, Acta Crystallogr. Sect. B **33**, 1773 (1977).

[9] H. Terauchi, T. Sakai, and H. Chihara, J. Chem. Phys. **62**, 3832 (1975); H. Chihara and N. Nakamuma, J. Phys. Soc. Jpn. **44**, 1567 (1978).

[10] A. Yoshihara, E. R. Bernstein, and J. C. Raich, J. Chem. Phys. **79**, 445 (1983).

[11] P. Toledano and J. C. Toledano, Phys. Rev. B **25**, 1946 (1982).

[12] J. C. Raich and E. R. Bernstein, J. Chem. Phys. **73**, 1955 (1980); A. Yoshihara, C. L. Pan, E. R. Bernstein, and J. C. Raich, *ibid.* **76**, 3218 (1982).

[13] A. Yoshihara, W. D. Wilber, E. R. Bernstein, and J. C. Raich, J. Chem. Phys. **76**, 2064 (1982); A. Yoshihara, E. R. Bernstein, and J. C. Raich, *ibid.* **77**, 2768 (1982); **79**, 2504 (1983).

[14] F. Jona and G. Shirane, *Ferroelectric Crystals* (Pergamon, New York, 1962).

[15] R. Nowak, Ph.D. thesis, Wrocław, Poland, 1984 (unpublished).

[16] V. Chandrasekhran, Proc. Indian Acad. Sci. Sec. A **33**, 183 (1951).

[17] E. Dieulesaint and D. Royer, *Ondes Elastiques dans les Solides* (Masson, 1974).

[18] C. J. Bradley and A. P. Cracknell, *The Mathematical Theory of Symmetry in Solids* (Clarendon, Oxford, 1972).

[19] G. Ya. Lubarskii, *The Application of Group Theory in Physics* (Pergamon, New York, 1960).

[20] W. Yao, H. Z. Cummins, and R. H. Bruce, Phys. Rev. B **24**, 424 (1981).

[21] R. Blinc and B.Žekš, *Soft Modes in Ferroelectrics and Antiferroelectrics* (Elsevier, Amsterdam, 1974).

[22] F. Schwabl, Phys. Rev. B **7**, 2038 (1973).

[23] L. D. Landau and I. M. Khalatnikov, Dokl. Akad. Nauk **96**, 469 (1954).

[24] A. Yoshihara, J. C. Burr, S. M. Mudare, E. R. Bernstein, and J. C. Raich, J. Chem. Phys. **80**, 3816 (1984).

[25] P. W. Young and J. F. Scott, Ferroelectrics **52**, 35 (1983).

[26] M. Zhang, T. Yagi, W. F. Oliver, and J. F. Scott, Phys. Rev. B **33**, 1381 (1986).